Available online at www.sciencedirect.com
SCIENCE DIRECT®
Journal of Solid State Chemistry 177 (2004) 4205–4212
JOURNAL OF SOLID STATE CHEMISTRY
www.elsevier.com/locate/jssc

Electrochemical approach to evaluate the mechanism of photocatalytic water splitting on oxide photocatalysts

Yasumichi Matsumoto[a], Ugur Unal[a,*], Noriyuki Tanaka[a], Akihiko Kudo[b], Hideki Kato[b]

[a]*Faculty of Engineering, Department of Applied Chemistry, Kumamoto University, Kurokami 2-39-1, Kumamoto-shi, Kumamoto-ken, 860-8555, Japan*
[b]*Faculty of Science, Science University of Tokyo, 1-3 Kagurazaka, Shinjuku-ku, Tokyo 162-8601, Japan*

Received 12 May 2004; received in revised form 28 July 2004; accepted 2 August 2004

Abstract

Photoelectrochemical measurements of TiO_2, $NaTaO_3$, and Cr or Sb doped TiO_2 and $SrTiO_3$ photocatalysts were carried out in H_2 and O_2 saturated electrolytes in order to evaluate the reverse reactions during water photolysis. The poor activity of TiO_2 as a result of reverse photoreactions of O_2 reduction and H_2 oxidation was revealed with the respective high cathodic and anodic photocurrents. The rise in the photocurrents at $NaTaO_3$ after La doping was in harmony with the doping-induced increase in the photocatalytic activity. NiO loading suppresses the O_2 photoreverse reactions, which declines photocatalytic activity, and/or promotes the photo-oxidation of water, because the O_2 photo-reduction current was scarcely observed near the flatband potential. Photocurrents of O_2 reduction and H_2 oxidation were observed under visible light for the Cr and Sb doped $SrTiO_3$ and TiO_2, respectively. These phenomena are in harmony with the previous reports on the photocatalysts examined with sacrificial reagents.

Keywords: Photochemistry; Water splitting; Reverse reactions; TiO_2; Oxide photocatalyst; Water photolysis; Oxide films; Semiconductor/solution interface; Doping

1. Introduction

Many researches on water splitting into hydrogen and oxygen molecules by semiconductor photocatalyst have been carried out since Honda-Fujishima principle [1], where the produced hydrogen is a prospective fuel because of no production of CO_2 after its oxidation. The water photolysis is a conversion system from solar energy to chemical fuel of hydrogen, only when photocatalyst responds to visible light. Currently, the high conversion efficiency has been discovered for some photocatalysts, however, as a result of the UV light response [2–7]. The photocatalysts that can use visible light with high conversion efficiency must be discovered and/or developed in the viewpoint of the energy conversion using solar energy.

The mechanism of the water photolysis has been mainly discussed from the viewpoint of the band structure and its energy positions. The electrochemical measurements are very useful for the evaluation of the photocatalytic mechanism, because the energy positions of the band edges of the conduction and valence bands are estimated from the results of the electrochemical measurements. The evaluation of the reverse reaction from hydrogen and oxygen to water under illumination is also important to clear the mechanism of the water photolysis, since the reverse reaction brings about the low conversion efficiency of the water photolysis on the photocatalyst. However, the electrochemical investigation of the reverse reactions, i.e., electrochemical hydrogen oxidation and oxygen reduction under illumination, has been scarcely made until now.

The electrochemical research is difficult, if the photocatalyst is an insulator. Therefore, only semiconductor samples with relatively high conductivity have

*Corresponding author. Fax: +81-96-342-3679.
E-mail address: 016d9573@gsst.stud.kumamoto-u.ac.jp (U. Unal).

0022-4596/$ - see front matter © 2004 Elsevier Inc. All rights reserved.
doi:10.1016/j.jssc.2004.08.001

been used in the electrochemical measurements. However, the electrochemical tests can be performed for the deposited low conductive photocatalyst particles on the metal substrate, when the very fine particles are in contact with substrate, because the total resistivity of the photocatalyst is not so large. In this principle, the measurement of photoelectrochemical properties is succeeded for some low conductive layered oxides in order to measure the electrochemical properties [8,9].

In this paper, the photoelectrochemical properties of TiO_2 with standard properties, $NaTaO_3$ with high quantum efficiency under UV light illumination [7,10], and doped TiO_2 and $SrTiO_3$ with visible light response in the water photolysis [11] are demonstrated. The results give some important evaluation in the photocatalytic mechanism. The above principle in preparing the electrode is applied, because the conductivities of almost all the samples are very low. Consequently, an electrophoretic deposition (EPD) technique is used to prepare the photocatalyst electrodes.

2. Experimental section

The photocatalyst powders used in this study were TiO_2 (*P*25, Degussa Co., Ltd., 30 nm average particle size), TiO_2 and $SrTiO_3$ doped with either Cr or Sb, $NaTaO_3$, $NaTaO_3$ doped with La(2%), and their NiO loaded samples. The powders except *P*25, were prepared by the same methods as described in previous papers [7,10,11]. The powders were fixed on the Au or ITO substrate by an electrophoretic deposition (EPD) technique [8,9] in acetone/I_2 solution. After the deposition, the deposited films were heated at 500 °C on certain occasions in order to increase in adhesion between the powder and the substrate. The sample powders used in this study are listed in Table 1.

The model of the photocatalyst deposited electrode is illustrated in Fig. 1. The ohmic drop due to the photocatalyst is neglected for the deposited particle size finer than about few μm. The voltage difference due to the ohmic drop is only 10 mV under 0.1 mA for a particle with few μm, when the specific resistivity is $10^7\,\Omega$ cm (TiO_2: $10^7\,\Omega$ cm [12]). Therefore, the electrochemical properties can be measured for the present photocatalysts, because the particle sizes are smaller than about few μm and the measured photocurrent are smaller than about 0.1 mA in general.

The morphology of the deposited films was observed by SEM. All electrochemical experiments were carried out in a conventional three-electrode electrochemical quartz cell with a Pt counter electrode and a saturated Ag/AgCl reference electrode. 0.1 M K_2SO_4 solution (pH = 6.4) was used as an electrolyte. The working electrode potentials were referred to this reference electrode unless otherwise stated in this paper. A 500 W ultra-high pressure Hg lamp was used as the light source to measure the photoelectrochemical properties. Cyclic voltammograms (CV) were measured under potential sweep rate of 20 mV s^{-1}. Electrolyte was saturated with N_2, O_2, or H_2 prior to the electrochemical measurements. The apparent porous film thickness of all the samples were about 3–8 μm, where the maximum photocurrents were observed.

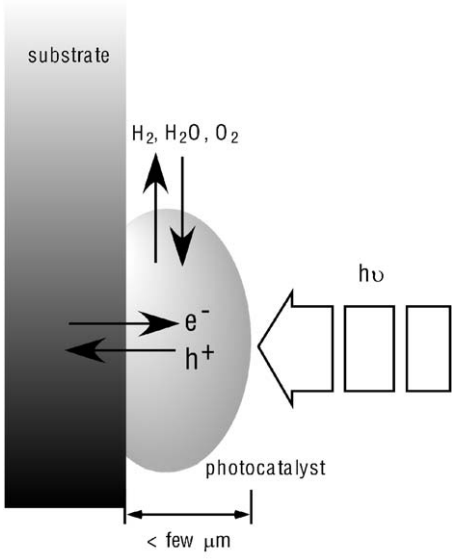

Fig. 1. Model of the electrode deposited with the photocatalyst.

Table 1
Band gaps and particle sizes of the photocatalysts

Catalyst	Cocatalyst	Band gap/eV	Particle size/μm
TiO_2(P25)	None	3.0	0.03
$NaTaO_3$	None	4.0	2–4
	NiO (0.05 wt%)		
$NaTaO_3$, La(2%)	None	4.1	0.1–0.7
	NiO (0.05 wt%)		
TiO_2, Sb(3%) + Cr(2%)	None	2.2	0.7–0.8
$SrTiO_3$, Sb(1.25%) + Cr(0.05%)	None	2.4	1–1.5

3. Results and discussion

3.1. Model of the simple electron and hole transfers at the semiconductor (photocatalyst)/solution interface for water photolysis

Oxygen and hydrogen evolved at a photocatalyst under illumination partially reacts to water (reverse reaction) in the water photolysis process. Therefore, photoelectrochemical reactions of oxygen and hydrogen should be measured in order to evaluate the above reverse reaction mechanism. Fig. 2 shows a basic model of the photoelectrochemical process at the semiconductor/solution interface, where water, hydrogen, and oxygen electrochemical reactions are illustrated as the plots of V vs. log i (based on Tafel equation). RHE, ROE, RC, and SS denote reversible hydrogen electrode, reversible oxygen electrode, recombination center in bulk (and/or in space charge layer), and surface state, respectively. i_H and i_O denote exchange current densities of hydrogen and oxygen electrochemical reactions respectively, and the former is much larger than the latter in general. Some excited electrons in the conduction band (CB) flow to the surface, and then react with H_2O and/or O_2 at the CB band-edge and/or the SS where some electrons recombine. The reacted electrons bring about the cathodic photocurrents of O_2 and H_2O at the CB band-edge (circle symbols) an/or via the SS (triangle symbols), which correspond to the related log i. The similar phenomena also occur for the produced hole in the valence band (VB), where the occurrence of H_2 and H_2O oxidation brings about the related log i in this figure (open symbols). In general, it is concluded that the evolved H_2 and O_2 easily react with electron and hole respectively rather than H_2O, because the currents of H_2 oxidation and O_2 reduction are larger than those of H_2O oxidation and reduction, respectively, due to the larger driving forces for the former reactions. However, this conclusion may sometimes not fit for some electrode surfaces, because the V–log i curve depends on the electrocatalytic activity of the electrode surface. For example, the electrochemical oxidation rate of H_2 and reduction rate of O_2 will be lower than those of H_2O, if the electrocatalytic activities of an electrode surface are relatively large for the latter reactions rather than the former reactions. Moreover, Fig. 2 illustrates only the simple case, where the site for the electron transfer for H_2O reduction to produce H_2 is the same as that for the hole transfer for H_2 oxidation to produce H_2O, and that for the hole transfer for H_2O oxidation to produce O_2 is the same as that for the electron transfer for O_2 reduction to produce H_2O. The real mechanism might be that the paths for both sites mentioned above are different from each other.

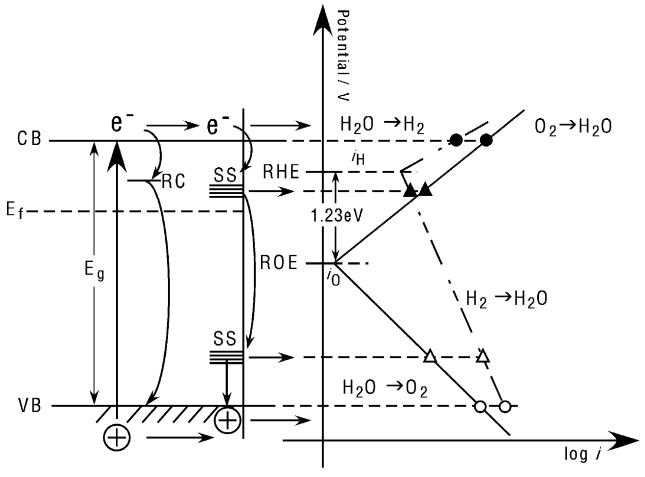

Fig. 2. Model of the mechanism of electron and hole transfers in the photocatalytic water splitting.

3.2. TiO_2 electrodes

Fig. 3(A) shows the voltammograms of the TiO_2/Ti electrode, which was prepared by the heat-treatment of Ti plate in air at 500 °C. The changing point of photocurrent (from cathodic photocurrent to anodic photocurrent or vice versa) in potential approaches to the flat band potential (V_{fb}). The V_{fb} was about –0.8∼–0.7 V, although it slightly depended on the direction of the potential sweep and the saturated gas. The V_{fb} measured in the present study was closely in agreement with those reported already.

The large O_2 reduction currents (cathodic photocurrent and dark current) were observed in the O_2 saturated electrolyte. The same result has been already reported by Lindquist et al. [13]. They proposed a mechanism that the cathodic photocurrent is based on the photoconduction of TiO_2 together with a redox couple (O_2/O_2^-) species existing on the surface, which collects the electrons in the conduction band. Evidently, the formation of cathodic photocurrent takes place under the presence of oxidants. Surface O_2 molecules contribute to the photo-induced current by trapping the electrons produced under illumination on the surface of the electrode. In addition, the contribution of the photo-induced current developed in low conductive regions to the observed photocurrent was also reported. Photo-induced current was assigned to the increase in the free charge carriers as a result of the excitation in the sub-band gap states, and subsequent increase in conductivity, which might, also, be the case for the current study [13].

Under O_2 saturation, a large anodic photocurrent in the potential region from the V_{fb} to about 0 V was observed in the sweep direction from negative to positive potential, but not in the reverse direction from positive to negative potential. The above anodic photocurrent is

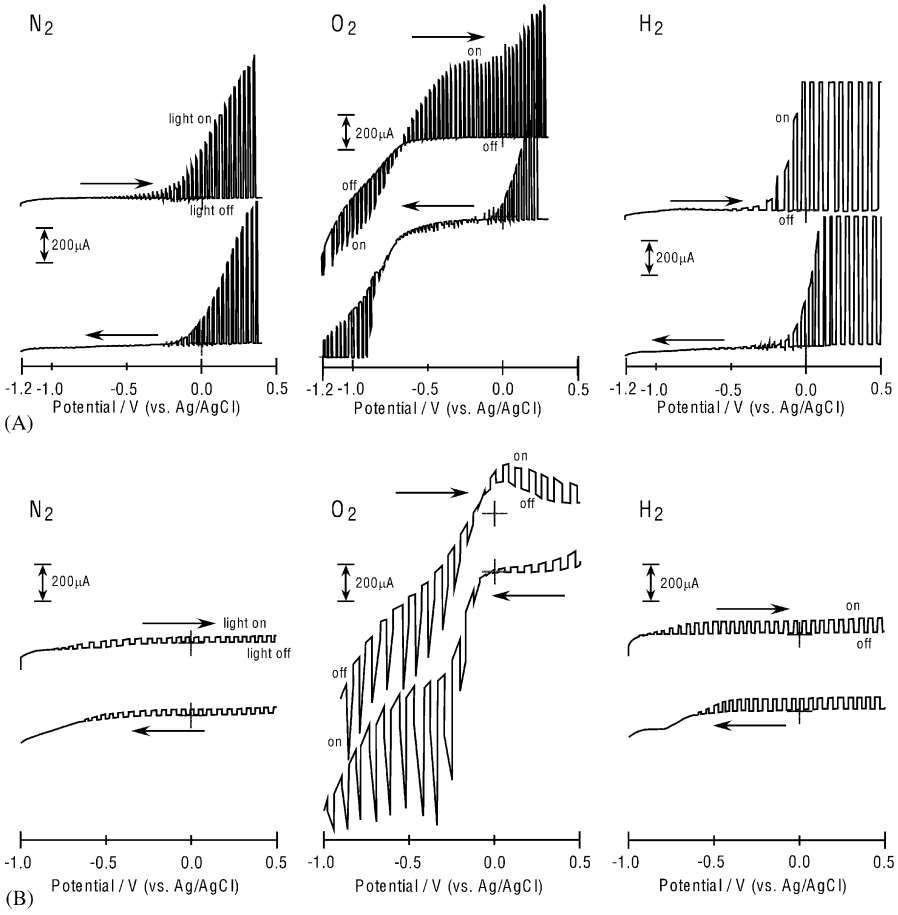

Fig. 3. Cyclic voltammograms of the TiO_2/Ti electrode (A) and TiO_2(*P*25)/Au electrode (B) in N_2, O_2, and H_2 saturated electrolytes under UV illumination. The horizontal arrows show the potential sweep directions.

based on the photo-oxidation of the adsorbed H_2O_2 (or O_2H^-) produced by the cathodic photo-reduction of O_2, because the same anodic photocurrent was observed after the addition of H_2O_2 into the electrolyte. The disappearance of the anodic photocurrent in the reverse sweep from positive to negative is based on the consumption of the adsorbed H_2O_2 by the anodic photo-oxidation in the sweep from negative to positive potential. In the case of H_2 saturated electrolyte, a large anodic photocurrent was observed in the potential region more positive than about 0 V compared with the case of N_2 saturation, but no increase in the anodic photocurrent in the potential region from the V_{fb} to about 0 V. Consequently, both large photocurrents in O_2 and H_2 saturated electrolytes compared with the case of N_2 saturation mean that the reduction of O_2 and oxidation of H_2 proceed more preferentially than those of H_2O because of the large driving forces for the former reactions regardless of the photoconduction and surface mechanisms.

Fig. 3(B) shows the voltammograms of the TiO_2(*P*25)/Au electrode. This TiO_2 electrode has the following phenomenon different from the above TiO_2/Ti electrode, although higher photocurrents in O_2 and H_2 saturated electrolytes than that in N_2 saturated one were observed as similar to the TiO_2/Ti electrode. The changing point of photocurrent shifts to more positive in O_2 (about −0.1 V). The similar phenomenon has been reported by Tsujiko et al. for nanometer size TiO_2 particle electrode, and explained by the adsorption of O_2 [14]. The present positive shift may be explained by the same mechanism such as O_2 and/or H_2O_2 adsorption. Oxygen molecules adsorbed on the surface of the TiO_2 film captures the surface conduction band electrons before they reach to the substrate. The phenomenon brings about decay in the anodic current as the cathodic current develops and becomes dominant even at a sufficiently more positive voltage. The shift to the positive energy may also be explained by the alteration in the energy levels on the surface as a result of charge accumulation.

In conclusion, the poor photocatalytic activity of TiO_2 for the water photolysis can be explained by high reverse reactions of the photo-reduction of the evolved O_2 and H_2O_2, and the photo-oxidation of the evolved H_2O_2 and H_2, even if H_2 and O_2 were evolved under UV light initially. The observed anodic and cathodic photocurrent, thus, can be assigned to these dominant

reverse reactions rather than the occurrence of the photoconduction under illumination.

3.3. $NaTaO_3$ electrodes with and without NiO loading

Figs. 4(A) and (B) show the voltammograms of the $NaTaO_3$ electrode and that loaded with NiO respectively. Photocurrents were observed for both electrodes in the electrolytes saturated with N_2, O_2, and H_2. The V_{fb} (which sets around the changing potential from anodic photocurrent to cathodic photocurrent) of the $NaTaO_3$ was about 0 V, while that of $NaTaO_3$ loaded with NiO was about 0.4 V. Thus, the V_{fb} shifted to positive by the NiO loading. It is estimated from Ref. [15] that the CB will be positioned at potentials more negative than RHE. Therefore, the energy difference between the Fermi level and the CB must be larger than about 1.0 eV for all the present $NaTiO_3$ samples. In the O_2 saturated electrolyte, cathodic photocurrent larger than that in the N_2 saturated electrolyte was observed for both electrodes, while the anodic photocurrent in the H_2 saturated electrolyte was almost same as that in the N_2 saturated electrolyte. Figs. 5(A) and (B) show the voltammograms of La doped $NaTaO_3$ (2% La) and that loaded with NiO electrodes, respectively. The photocurrents larger than those in the non-doped $NaTaO_3$ (Fig. 4) were observed for the La doped samples, although the same phenomena with the cases of the non-doped $NaTaO_3$, i.e., positive shift of the V_{fb} by about 0.4 V by NiO loading, and the increase of the cathodic photocurrent in the O_2 saturated electrolyte were observed. Especially, the pronounced increase in the cathodic photocurrent in the O_2 saturated electrolyte occurred in the potential region where the oxygen reduction current at the Au substrate electrode appeared in the dark. Some H_2O_2 produced in this potential region somewhat will affect the increase in the cathodic photocurrent, because the relatively large photo-reduction current was observed in the H_2O_2 added electrolyte. Simultaneously, a slight increase in the anodic photocurrent was also observed in the electrolyte with H_2O_2. Therefore, sweeping the potential from positive to negative direction is practically more preferable in order to decrease the effect of the produced H_2O_2.

The comparisons between the photocurrents of O_2, N_2, and H_2 near the V_{fb} are very important to evaluate the mechanism of the photocatalyst in water photolysis, because the reaction at the photocatalyst proceeds at a potential near the V_{fb} (In fact, the rest potentials of all the electrodes under the illumination were near the V_{fb}). The photocurrent ratios of I_O/I_{NC} and I_H/I_{NA} are listed in Table 2, where I_O, I_{NC}, I_{NA}, and I_H denote the cathodic photocurrent in the O_2 saturated electrolyte that in the N_2 saturated electrolyte, the anodic photocurrent in the N_2 saturated electrolyte, and the anodic photocurrent in the H_2 saturated electrolyte, respectively. Each photocurrent was calculated from the voltammograms of the positive to negative potential scan in order to exclude the H_2O_2 effect as stated above. All ratios were approximated to the closest value, because of the errors in the calculated photocurrent values. The ratios of I_H/I_{NA} were lower than about 2–3 at the potential region more positive than the V_{fb}, indicating that photo-oxidation of H_2 scarcely occurs for all the $NaTaO_3$ samples. However, the ratios of I_O/I_{NC} were very large (>about 3–5) for the samples without NiO loading, but not large (< about 2–3) for the NiO loaded samples at potentials near the V_{fb}. This is very important to evaluate the NiO loading effect on the photocatalyst. That is, the NiO loaded into the

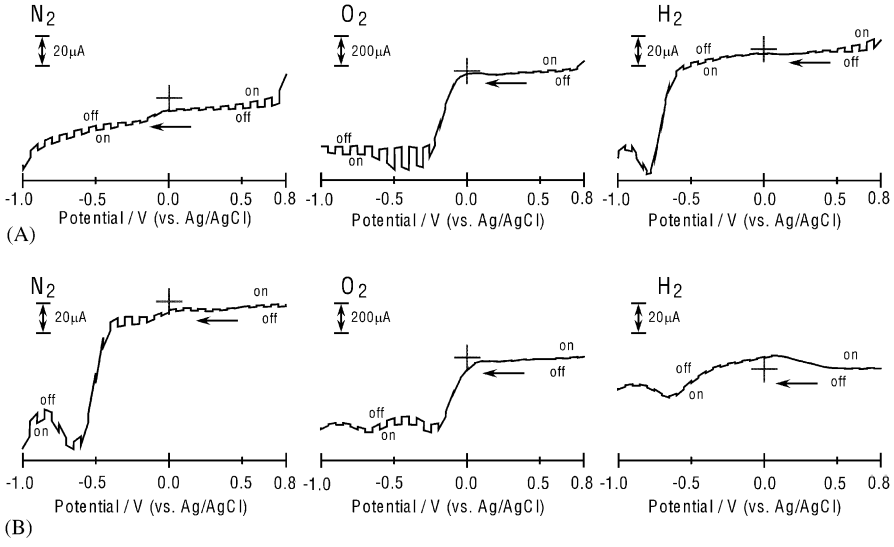

Fig. 4. Cyclic voltammograms of the $NaTaO_3$/Au electrode (A) and $NaTaO_3$:NiO/Au electrode (B) in N_2, O_2, and H_2 saturated electrolytes under UV illumination.

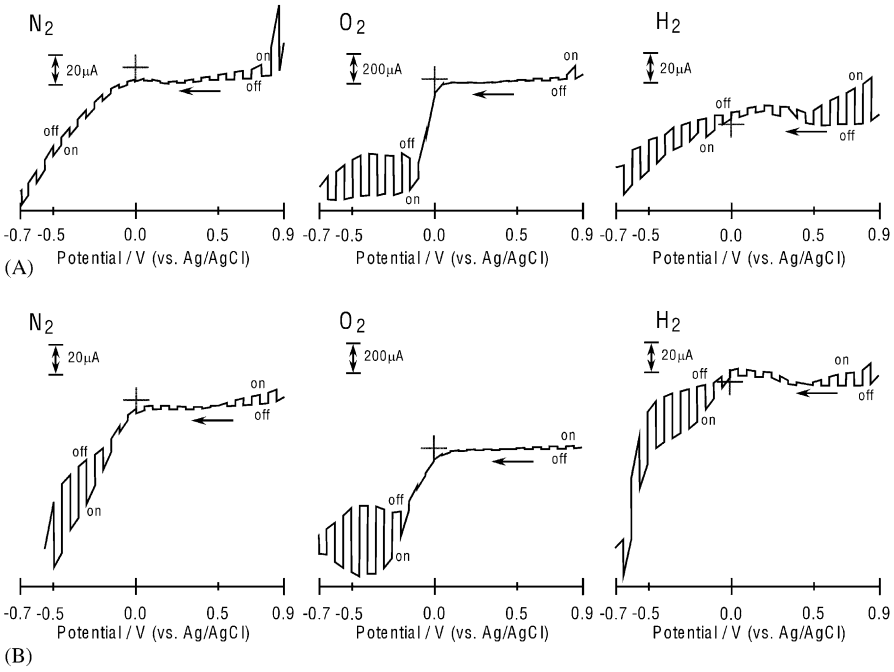

Fig. 5. Cyclic voltammograms of the $NaTaO_3$, La/Au electrode (A) and $NaTaO_3$, La:NiO/Au electrode (B) in N_2, O_2, and H_2 saturated electrolytes under UV illumination.

Table 2
Photocurrent ratios in the N_2, O_2, and H_2 saturated electrolytes for $NaTaO_3$ samples

Samples/substrate	V_{CP}		Potential/V vs. Ag/AgCl											
			−0.4	−0.3	−0.2	−0.1	0	0.1	0.2	0.3	0.4	0.5	0.6	0.7
$NaTaO_3$/Au	0	I_O/I_{NC}	> 50	50–60	30–50	30–50	—	—	—	—	—	—	—	—
		I_H/I_{NA}	—	—	—	—	—	—	0	0.1–0.2	0.3–0.5	0.6–0.8	1.1	1.2
$NaTaO_3$/ITO	0.1	I_O/I_{NC}	14–15	5–6	4–5	3–4	3–4	—	—	—	—	—	—	—
$NaTaO_3$:NiO/Au	0.4	I_O/I_{NC}	8–10	12–13	15–17	7–8	1–2	1–2	1–2	1–2	—	—	—	—
		I_H/I_{NA}	—	—	—	—	—	—	—	—	—	0–1	1	1.2
$NaTaO_3$:NiO/ITO	0.2–0.3	I_O/I_{NC}	3–4	1.9–2.0	~1.5	~1	~0.5	0–0.2	—	—	—	—	—	—
$NaTaO_3$, La/Au	0–0.3	I_O/I_{NC}	80–90	50–60	60–70	30–50	—	—	—	—	—	—	—	—
		I_H/I_{NA}	—	—	—	—	—	2–3	2–3	2–3	2–3	2–3	2–3	3–4
$NaTaO_3$,La/ITO	−0.1–0	I_O/I_{NC}	10–11	10–15	20–30	—	—	—	—	—	—	—	—	—
$NaTaO_3$,La:NiO/Au	0.4	I_O/I_{NC}	12–13	12–13	10–12	3–4	2–3	2–3	2–3	2–3	—	—	—	—
		I_H/I_{NA}	—	—	—	—	—	—	—	—	—	—	1–2	1–2
$NaTaO_3$,La:NiO/ITO	0.2–0.3	I_O/I_{NC}	1–2	1–2	1–2	1–2	1–2	1–2	—	—	—	—	—	—

Note. V_{CP}: the potential where photocurrent changes near V_{fb}.

samples suppresses the O_2 photo-reduction and/or promotes the H_2O photo-reduction.

In conclusion, O_2 photo-reduction rather than H_2 photo-oxidation as the reverse reaction in the photolysis of water occurs on the $NaTaO_3$, leading to the decrease in the quantum efficiency. La doping will bring about the suppression of the recombination in the bulk and/or at surface, and increase the quantum efficiency. This will be estimated from the increase in the photocurrents by the La doping. Moreover, the O_2 photo-reduction was relatively suppressed by the NiO loading. This will lead to a high quantum efficiency for the water photolysis at the La doped $NaTaO_3$ loaded with NiO. The effects of the NiO loading were disappeared by heat-treatment at 500 °C in air, suggesting that the oxidized NiO will not sufficiently act as a promoter in the water photolysis.

3.4. Cr, Sb doped TiO_2 and $SrTiO_3$ electrodes

Figs. 6(A) and (B) show the voltammograms of the Cr and Sb doped TiO_2 and $SrTiO_3$ samples measured under illumination of the visible light (>420 nm), respectively.

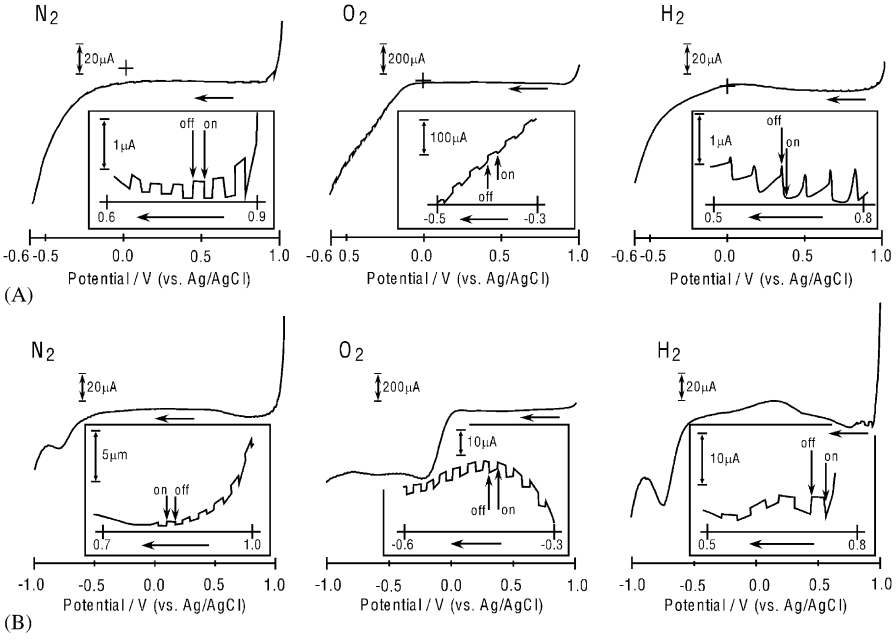

Fig. 6. Cyclic voltammograms of the TiO_2, Sb + Cr/Au electrode (A) and $SrTiO_3$, Sb + Cr/Au electrode (B) in N_2, O_2, and H_2 saturated electrolytes under visible light illumination. Insets show the magnified region of interest.

Table 3
Photocurrent ratios in the N_2, O_2, and H_2 saturated electrolytes under illumination of visible light for TiO_2,Sb + Cr/Au and $SrTiO_3$,Sb + Cr/Au samples

Samples/Substrate	V_{CP}		Potential/V vs. Ag/AgCl												
			−0.4	−0.3	−0.2	−0.1	0	0.1	0.2	0.3	0.4	0.5	0.6	0.7	0.8
$SrTiO_3$,Sb + Cr/Au	0.2–0.3	I_O/I_{NC}	25	13.3	50	—	—	—	—			—	—	—	—
		I_H/I_{NA}	—	—	—	—	—	—	0		1–2	1–2	1–2	1–2	5
TiO_2,Sb + Cr/Au	0.5	I_O/I_{NC}	—	—	2–3	0.5–1	0.5–1	1	1	1	—	—	—	—	—
		I_H/I_{NA}	—	—	—	—	—	—	—	—	—	—	10–20	10–20	10–20

Note. V_{CP}: the potential where photocurrent changes near V_{fb}.

These photocatalysts showed visible light response in photocurrent. These phenomena are in harmony with the photocatalytic activity under visible light for these samples [11]. It was reported that transition metal ions codoped with Sb have a significant contribution to the adsorption bands observed in visible light region for TiO_2 and $SrTiO_3$. Photocatalytic activities by band gap activation was enhanced by Sb–Cr doping. In these electrodes, Cr^{3+} created electron donor centers in TiO_2 but discrete levels in $SrTiO_3$. In order to prevent the formation of recombination centers, Sb^{5+} was codoped as a charge balance agent [11]. Table 3 lists the ratios of I_O/I_{NC} and I_H/I_{NA}, where I_O, I_{NC}, I_{NA}, and I_H denote the cathodic photocurrent in the O_2 saturated electrolyte, that in the N_2 saturated electrolyte, the anodic photocurrent in the N_2 saturated electrolyte, and that in the H_2 saturated electrolyte under the visible light, respectively. In the case of the TiO_2 sample, the ratios of I_O/I_{NC} were lower than about 1, indicating that the O_2 photo-reduction scarcely occurs. On the other hand, the ratios of I_H/I_{NA} were higher than about 10, indicating that the H_2 photo-oxidation occurs more easily than H_2O. Consequently, water photolysis under visible light scarcely occurs by the H_2 photo-oxidation. At this sample, O_2 evolution has been observed by the Ag^+ addition, but not H_2 evolution by the methanol addition [11]. These phenomena are explained by the H_2 photo-oxidation, because the evolved H_2 is immediately photo-oxidized at the catalyst surface.

In the case of the $SrTiO_3$ sample, the ratios of I_O/I_{NC} were larger than about 10 while those of I_H/I_{NA} were smaller than about 2–3. These results indicate that the O_2 photo-reduction preferentially occurs but not the H_2 photo-oxidation under visible light. Consequently, water photolysis does not occur by the preferential photo-reduction of O_2 under illumination of the visible light. H_2 evolution after the addition of methanol and very low amount of O_2 evolved after the addition of

Ag^+ can be explained by the preferential photo-reduction of the evolved O_2 [11].

4. Conclusions

Photoelectrochemical measurements of the photocatalysts such as TiO_2, $NaTaO_3$, TiO_2 and $SrTiO_3$ doped with Cr and Sb, were carried out in the N_2, H_2 or O_2 saturated electrolytes in order to evaluate the reverse reactions. Photocatalyst powder deposited electrode were prepared by the EPD technique at Au or ITO substrates, where the ohmic drops due to the catalyst themselves will be negligible. It is concluded that O_2 photoreduction and H_2 photooxidation preferentially occurs in respectively O_2 and H_2 saturated electrolytes with larger cathodic and anodic photocurrents than those saturated with N_2.

The poor activity of TiO_2 is explained by both reverse photoreactions, because high anodic photocurrent of H_2 and high cathodic photocurrent of O_2 were observed. The increase in the photocurrents at $NaTaO_3$ as a result of La doping was in harmony with the doping-induced increase in the photocatalytic activity as a result of the La doping. Relatively high O_2 photo-reduction current was observed, but not for the H_2 photo-oxidation at the $NaTaO_3$ without NiO. In other words, the water photolysis on these catalysts is suppressed by the O_2 photo-reduction. On the other hand, the NiO loading brought about the suppression of the O_2 photo-reduction and/or the increase in the photo-oxidation of water, because the O_2 photo-reduction current was scarcely observed for the NiO loaded $NaTaO_3$ samples. Consequently, high photocatalytic activity of the NiO loaded $NaTaO_3$ doped with La [7] will be brought about by the negligible reverse reactions of H_2 and O_2. The O_2 photo-reduction and H_2 photo-oxidation currents were observed under visible light for $SrTiO_3$ and TiO_2 doped with Cr and Sb, respectively. These phenomena are also in harmony with the results of the photocatalysts in the presence of the sacrificial reagents reported already [11].

Acknowledgments

This work was supported by the Core Research for Evolutional Science and Technology (CREST) program of the Japan Science and Technology Co. (JST), and a Grant-in-Aid for Scientific Research (No 15350123) from the Ministry of Education, Culture, Sports, Science, and Technology.

References

[1] A. Fujishima, K. Honda, Nature 238 (1972) 37.
[2] A. Kudo, K. Sayama, A. Tanaka, K. Asakura, K. Domen, K. Maruya, T. Onishi, J. Catal. 120 (1989) 337.
[3] T. Tanaka, K. Shinohaya, A. Tanaka, M. Hara, J.N. Kondo, K. Domen, J. Photochem. Photobiol. A 106 (1997) 45.
[4] Y. Inoue, M. Kohno, T. Kaneko, S. Ogura, K. Sato, J. Chem. Soc. Faraday Trans. 94 (1998) 89.
[5] T. Ishihara, H. Nishiguchi, K. Fukamachi, Y. Takita, J. Phys. Chem. B 103 (1999) 1.
[6] M. Machida, J. Yabunaka, T. Kijima, Chem. Mater. 12 (2000) 812.
[7] H. Kato, K. Asakusa, A. Kudo, J. Am. Chem. Soc. 125 (2003) 3082.
[8] Y. Matsumoto, A. Funatsu, D. Matsuo, U. Unal, J. Phys. Chem. B 105 (2001) 10893.
[9] U. Unal, Y. Matsumoto, N. Tanaka, Y. Kimura, N. Tamoto, J. Phys. Chem. B 107 (2003) 12680.
[10] H. Kato, A. Kudo, J. Phys. Chem. B 105 (2001) 4285.
[11] H. Kato, A. Kudo, J. Phys. Chem. B 106 (2002) 5029.
[12] R.N. Viswanath, A. Chandra Bose, S. Ramasamy, J. Phys. Chem. Solids 62 (2001) 1991.
[13] S.E. Lindquist, H. Vidarsson, J. Molecul. Catal. 38 (1996) 131–155.
[14] A. Tsujiko, H. Itoh, T. Kisumi, A. Shiga, K. Murakoshi, Y. Nakato, J. Phys. Chem. B 106 (2002) 5878.
[15] Y. Matsumoto, J. Solid State. Chem. 126 (1996) 227.